Available online at www.sciencedirect.com
SCIENCE DIRECT®
ELSEVIER
Applied Catalysis B: Environmental xxx (2006) xxx–xxx
APPLIED CATALYSIS B: ENVIRONMENTAL
www.elsevier.com/locate/apcatb

The origin of the enhanced activity of Pt/zeolites for combustion of C_2–C_4 alkanes

T.F. Garetto, E. Rincón, C.R. Apesteguía *

Catalysis Science and Engineering Research Group (GICIC), Instituto de Investigaciones en Catálisis y Petroquímica-INCAPE-(UNL-CONICET), Santiago del Estero 2654, (3000) Santa Fe, Argentina

Received 3 February 2006; received in revised form 10 June 2006; accepted 12 June 2006

Abstract

The deep oxidations of ethane, propane and butane were studied on Pt supported on MgO, alumina, and zeolites KL, HY, ZSM5, and Beta. The catalyst activities were evaluated through both conversion versus temperature (light-off curves) and conversion versus time catalytic tests. The Pt oxidation activity for the three lower alkanes was drastically increased when supported on zeolites as compared to Pt/Al_2O_3 or Pt/MgO. C_2–C_4 alkane oxidation turnover rates were about two (ethane, propane) and one (butane) orders of magnitude higher on Pt/acid zeolites than on Pt/Al_2O_3, but also weakly acid PtKL zeolite was significantly more active as compared to Pt/Al_2O_3 (more than one order of magnitude for ethane and propane). This latter result showed that the support acidity is not a major contributing factor for lower alkane combustion. Promotion of the alkane oxidation activity on Pt/zeolites was explained by considering the drastic increase observed for the density of alkane adsorbed species on zeolite supports; it was found, in fact, that the alkane uptake per m^2 was about one order of magnitude higher on Pt/zeolites than on Pt/Al_2O_3. This alkane confinement in zeolite pores would enhance the Pt oxidation rate because the reaction is positive order with respect to the hydrocarbon and probably also because would promote an additional oxidation pathway in the metal-oxide interfacial region.

Keywords: Lower-alkanes combustion; Pt-based catalysts; Zeolite supports; Confinement effect

1. Introduction

Hydrocarbon combustion has been widely studied on conventional Pt/Al_2O_3 catalysts because platinum is highly active for oxidative removal of small amounts of hydrocarbon from gaseous or liquid streams [1,2]. However, stable lower alkanes such as propane or ethane require relatively high temperatures to be completely oxidized over Pt/Al_2O_3 and increasing research work has been lately undertaken to find suitable supports for promoting the intrinsic Pt oxidation activity.

Several authors have observed that the Pt/Al_2O_3 activity for propane combustion may be increased by alumina sulfation [3–8]. This propane oxidation rate enhancement has been explained by considering that the formation of stable sulfate species at the Pt/support interface facilitates the dissociative chemisorption of propane and thereby enhances the intrinsic oxidation activity of platinum [5,6]. Other authors have suggested that formation of acidic sites at the $Pt/Al_2O_3/SO_4^{2-}$ interface generates a new reaction oxidation pathway consisting in the initial cracking of propane, forming ethane and a C_1 fragment [7]. Recently, Corro et al. [8] proposed that the promoting effect on propane combustion is due to the interaction of surface sulfates with surface highly oxidized Pt atoms that can be ascribed to Pt^{4+} at the edge of the Pt particles.

Yasawa et al. [9,10] studied the effect of support on propane oxidation activity by supporting Pt on MgO, Al_2O_3, SiO_2–Al_2O_3, and ZrO_2. They found that the catalytic activity of platinum is enhanced when the metal is supported on more acidic supports. The same authors studied the additive effect for propane combustion on Pt/Al_2O_3 by incorporating to the support several additives, such as Na, Cs, Ca, Mg, and Mo [11] and observed that propane oxidation activity on platinum increased with the increase in the electronegativity of additives. They explained these results by assuming that the oxidation-resistance of platinum under oxidizing conditions is enhanced by more acidic supports or more electronegative additives; preservation

* Corresponding author. Tel.: +54 342 4555279; fax: +54 342 4531068.
E-mail address: capesteg@fiqus.unl.edu.ar (C.R. Apesteguía).

0926-3373/$ – see front matter © 2006 Published by Elsevier B.V.
doi:10.1016/j.apcatb.2006.06.010

of Pt in metallic state would result in more active oxidation catalysts. However, other authors claimed that the support acid strength does not have a major influence on propane oxidation activity [4,5]. It is worth noting that in all these previous studies regarding the effect of support acidity on Pt activity for propane oxidation, authors did not use platinum supported on zeolitic materials.

Recently [12], we studied the deep oxidation of propane over Pt supported on MgO, Al_2O_3, and zeolites KL, HY, ZSM5, and Beta. Results showed that the propane oxidation turnover rate was more than two orders of magnitude higher on Pt/zeolites compared to Pt/Al_2O_3 catalyst. This drastic rate enhancement was essentially analyzed in terms of both support acidity and support capacity for adsorbing propane. In this paper, we have extended these studies by performing the oxidation of ethane and butane over the same catalysts used in [12], and by comparing the results with those obtained for propane oxidation. We will show that combustions of ethane, propane, and butane on Pt-based samples exhibit a similar catalytic behavior, and are drastically promoted on Pt/zeolites as compared to Pt/Al_2O_3. The superior activity of Pt/zeolites for alkane combustion is attributed to a significant increase of the density of alkane adsorbed species during reaction because of the alkane confinement in zeolite micropores.

2. Experimental

Chlorine-free Pt/Al_2O_3 catalyst was made by incipient-wetness impregnation at 303 K of a high-purity γ-Al_2O_3 powder (Cyanamid Ketjen CK300) with an aqueous solution of tetraamine platinum nitrate, $Pt(NH_3)_4(NO_3)_2$ (Alfa) for 6 h. The CK300 alumina has BET surface area (Sg) of 180 $m^2\ g^{-1}$, pore volume of 0.49 $cm^3\ g^{-1}$ and contains 50 ppm sulfur. The impregnated alumina was dried overnight at 393 K, then heated in air at 773 K for 4 h and finally reduced 4 h at 773 K in pure hydrogen. Three portions of Pt/Al_2O_3 catalyst were treated for 2 h in a 2% O_2/N_2 mixture at 868, 883, and 893 K, respectively, in order to sinter the metallic fraction and then reduced 4 h at 773 K; the resulting sintered catalysts are identified here as Pt/Al_2O_3-1, Pt/Al_2O_3-2, and Pt/Al_2O_3-3, respectively. Pt/MgO was prepared following the same procedure described for Pt/Al_2O_3; the MgO support was obtained by rehydration of a commercial MgO (Carlo Erba, 99%) as described elsewhere [13]. Platinum supported on HY zeolite (Pt/HY) was prepared by adding Pt by ion exchange. The HY zeolite was in turn obtained by exchanging a commercial NaY zeolite (UOP-Y 54, Si/Al = 2.4) with ammonium acetate (Sigma, 99%) at 298 K. HY zeolite was treated with deionized water at 343 K for 12 h in a stirred batch reactor and then an aqueous solution of $Pt(NH_3)_4(NO_3)_2$ was added dropwise. The sample was kept at 343 K for 12 h and then filtered, washed thoroughly with deionized water, and dried at 373 K overnight. Finally, Pt/HY was heated in air at 0.2 K min^{-1} from 298 up to 573 K and then reduced with flowing H_2 for 1 h at 673 K. Samples of Pt supported on zeolites Beta (Zeocat PB, Si/Al = 25), ZSM5 (Zeocat Pentasil PZ-2/54, Si/Al = 20) and KL (commercial Tosoh zeolite) were prepared following the same procedure used for Pt/HY.

The platinum dispersion (D_{Pt}) was determined by chemisorption of hydrogen and oxygen, (OC). Volumetric adsorption experiments were performed at 298 K in a conventional vacuum unit. Catalysts were reduced in H_2 at 673 K for 2 h and then outgassed 2 h at 773 K prior to performing gas chemisorption experiments. Hydrogen uptake was determined using the double isotherm method. After cooling to room temperature a first isotherm (primary isotherm) was drawn for measuring the total H_2 uptake. Then, and after 1 h of evacuation at room temperature, a second isotherm (secondary isotherm) was performed to determine the amount of weakly adsorbed H_2. The amount of irreversibly held H_2, $(HC)_i$, was calculated as the difference between total and weakly adsorbed H_2. The pressure range of isotherms was 0–6.6 kPa. In the case of oxygen chemisorption, a single isotherm was performed for determining (OC) values since the amount of reversible oxygen at room temperature was negligible. Stoichiometric atomic ratios of $(HC)_i/Pt_s = 1$ and $(OC)/Pt_s = 1$, where Pt_s implies a Pt atom on surface, were used to calculate the platinum dispersion. Mean Pt crystallite sizes ($\bar{d}_{Pt}$, Å) were determined from chemisorption data by using site densities of 1.12×10^{15} sites per cm^2 of metal [14].

Acid site densities were determined by using temperature programmed desorption (TPD) of NH_3. Samples (200 mg) were treated in He ($\sim$60 $cm^3\ min^{-1}$) at 773 K for 1.5 h and exposed to a 1.01% NH_3/He stream at 373 K until surface saturation. Weakly adsorbed NH_3 was removed by flowing He at 60 $cm^3\ min^{-1}$ for 0.5 h. Temperature was then increased to 823 K at 10 K min^{-1}, and the NH_3 concentration in the effluent was measured by mass spectrometry (MS) in a Baltzers Omnistar unit.

Alkane uptakes were measured at 298 K in conventional vacuum equipment. Samples were treated in air at 573 K for 0.5 h, then outgassed at this temperature for 1 h and finally cooled in vacuum to room temperature prior to performing the alkane adsorption isotherms.

Platinum loadings were measured by atomic absorption spectrometry. Total surface areas were measured by N_2 physisorption at 77 K using a Quantachrome Nova-1000 sorptometer and BET analysis methods.

Alkane oxidation reactions were carried out in a tubular paked bed reactor (Pyrex, 0.8 cm i.d.) at atmospheric pressure. Samples were sieved to retain particles with 0.35–0.42 mm diameter and loaded to the reactor. Zeolite powders were first pressed and compacted, and then crushed and screening to the desired size. Standard catalytic tests were performed at 101.3 kPa, using catalyst loadings (W) of 0.3 g, contact times of 58.0 (propane, W/F^0_P) and 22.4 (ethane, butane, $W/F^0_{E(B)}$) g catalyst h mol^{-1}, and gas flow rates (GHSV) of 1000 cm^3 (STP) $g^{-1}\ min^{-1}$. Gaseous mixture compositions were—propane:O_2:N_2 = 0.8:9.9:89.3 and ethane (butane):O_2:N_2 =1.8:10:88.2. On-line chromatographic analysis was performed using a gas chromatograph Shimadzu GC-8A equipped with a flame ionization detector and 23% SP-1700 Supelco packed columns. Before gas chromatographic analysis, the reaction products were separated and carbon dioxide converted to methane by means of a methanation catalyst (Ni/Kieselghur) operating at 673 K. Carbon monoxide was never detected in the

Table 1
Physical properties and acidity characterization of the catalysts

Catalyst	S_g ($m^2\ g^{-1}$)	Pt loading (%)	Pt dispersion D_{Pt} (%)	Mean Pt particle size $\bar{d}_{Pt}$ (Å)	NH_3 TPD ($\mu mol\ m^{-2}$)
Pt/MgO	140	0.40	35	24.2	n.d.[a]
Pt/Al_2O_3	180	0.33	53	16.0	0.11
Pt/KL	290	0.44	71	11.9	0.19
Pt/HY	440	0.32	40	21.1	1.03
Pt/ZSM5	400	0.36	30	28.2	0.89
Pt/Beta	560	0.33	29	29.2	0.86
Pt/Al_2O_3-1	180	0.33	42	20.1	–
Pt/Al_2O_3-2	180	0.33	22	38.4	–
Pt/Al_2O_3-3	180	0.33	19	44.5	–

[a] n.d.: not detected.

effluent. Before catalytic measurements, all the catalysts were reduced in hydrogen at 673 K for 1 h and then cooled to the desired temperature. Two experimental procedures were used for catalyst testing. Deep alkane oxidation was studied by obtaining curves of hydrocarbon conversion (X) as a function of temperature (light-off curves). The temperature was raised by steps of about 20 K, from 373 to 850 K. Kinetically-controlled X versus time tests were performed at constant temperature: 523 K (propane), 573 K (ethane), and 438 K (butane). In all the cases, alkane conversion was lower than 10%. The products were sampled at 5 min intervals using an automated sampling valve.

3. Results and discussion

3.1. Catalyst characterization

Table 1 shows the metal characterization and the values of BET surface area for the samples used in this work. The amount of Pt was between 0.32 and 0.44% on all the catalysts. The mean Pt particle sizes shown in Table 1 were calculated from D_{Pt} values determined by H_2 chemisorption; selected samples were also characterized by O_2 chemisorption. Table 1 shows that the Pt particle size on fresh catalysts varied between 16 and 29.2 Å, excepting for Pt/KL ($\bar{d}_{Pt} = 11.9$ Å).

The sample acid properties were probed by TPD of NH_3 preadsorbed at 373 K. The obtained NH_3 TPD profiles were presented in a previous work [12] and showed that on Pt/Al_2O_3 and Pt/KL ammonia desorbs in a band between 425 and 550 K. Acid zeolites contained a higher density of stronger acid sites compared to zeolite KL or Al_2O_3, and ammonia desorbed in two or three broad bands, from 425 to 800 K, on Pt/HY, Pt/Beta, and Pt/ZSM5 samples. The amount of NH_3 desorbed from Pt/MgO was negligible. The NH_3 surface densities were obtained by deconvolution and integration of the TPD traces and are presented in Table 1. The total adsorbed NH_3 surface densities on Pt/HY (0.86 $\mu mol\ m^{-2}$), Pt/ZSM5 (0.89 $\mu mol\ m^{-2}$), and Pt/Beta (1.03 $\mu mol\ m^{-2}$) were significantly higher compared to those on Pt/Al_2O_3 (0.11 $\mu mol\ m^{-2}$) and Pt/KL (0.19 $\mu mol\ m^{-2}$).

3.2. Catalytic results

The light-off curves obtained for combustion of ethane and butane on all the samples using a contact time of $W/F^0_{E(B)} = 22.4\ g\ h\ mol^{-1}$ are shown in Fig. 1. It is observed that on a given sample butane oxidation starts at lower temperatures as compared to ethane; for example, the initial butane oxidation temperature on acid zeolites is about 713 K while ethane oxidation begins at temperatures higher than 773 K. This is on line with previous results showing that the alkane oxidation rate on platinum increases with increasing the hydrocarbon chain length [15,16], and is consistent with the proposal that alkane oxidation is limited by the initial H abstraction, because the easy of breaking the C–H bond increases in the same order [15,17–19]. Besides, Fig. 1 also shows that the catalyst oxidation activity for both reactants follows the order $Pt/MgO < Pt/Al_2O_3 < Pt/KL < Pt/HY < Pt/ZSM5 < Pt/Beta$. The same activity trend was observed for propane. To quantitatively compare the

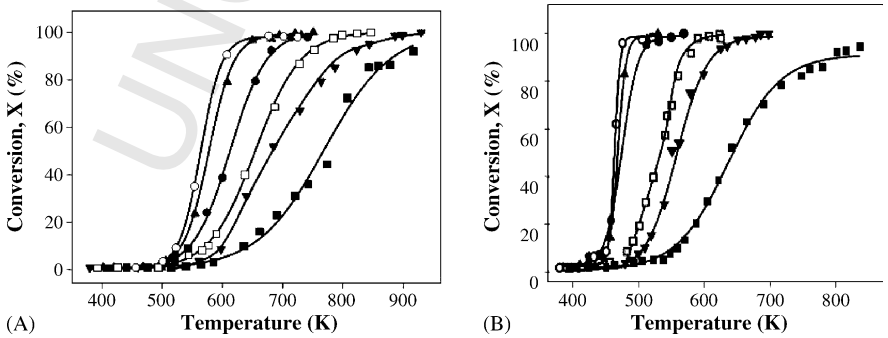

Fig. 1. Light-off curves for ethane (A) and butane (B) combustions. Pt/Beta (○); Pt/ZSM5 (▲); PtHY (●); Pt/KL (□); Pt/Al_2O_3 (▼); Pt/MgO (■). Conditions: $P = 101.3$ kPa, $W/F^0_{E(B)} = 22.4\ g\ h\ mol^{-1}$; ethane (butane):$O_2$:$N_2$ = 1.8:10:88.2.

Table 2
Sample activity for alkane combustion obtained from light-off curves and X vs. t catalytic tests

Catalyst	Ethane		Propane		Butane	
	T^{50} (K)[a]	TOF (h^{-1})[b]	T^{50} (K)	TOF (h^{-1})	T^{50} (K)	TOF (h^{-1})
Pt/MgO	769	100	715	30	643	n.d
Pt/Al_2O_3	661	200	630	85	553	30
Pt/KL	631	2800	580	1400	528	100
Pt/HY	578	15000	525	9000	468	200
Pt/ZSM5	564	22000	500	10000	463	320
Pt/Beta	528	60000	485	39000	460	550

[a] Values determined from light-off curves. $P = 101.3$ kPa, $W/F^0_{E(B)} = 22.4\ g\,h\,mol^{-1}$; ethane (butane):$O_2$:$N_2$ = 1.8:10:88.2, $W/F^0_P = 58.0\ g\,h\,mol^{-1}$; propane:$O_2$:$N_2$ = 0.8:9.9:89.3.
[b] Turnover frequencies determined from X vs. t tests at 438 K (butane), 523 K (propane), and 573 K (ethane). W/F^0 was selected to maintain X lower than 10% on all the samples. $P = 101.3$ kPa, ethane (butane):O_2:N_2 = 1.8:10:88.2, propane:O_2:N_2 = 0.8:9.9:89.3.

oxidation catalyst activity, we measured from light-off curves the value of the temperature at $x = 50\%$ (T^{50}). The obtained T^{50} values on all the samples for ethane, propane, and butane are given in Table 2. Table 2 shows that T^{50} decreased following the activity trend established above from 769 (Pt/MgO) to 528 K (Pt/Beta) for ethane, from 715 to 485 K for propane, and from 643 to 460 K for butane. On the other hand, we note here that two consecutive light-off curves for propane combustion were performed on Pt/Al_2O_3 and Pt/Beta, respectively. The difference in the oxidation activity between both samples determined from the respective first catalytic runs was maintained when observing the second catalytic curves; i.e., the activity relationships between both catalysts were sustained.

Alkane oxidation was also investigated by performing X versus t catalytic tests, at constant temperature. The initial conversion was kept lower than 10% on all the catalysts and the reaction was kinetically controlled. In Fig. 2 we have plotted ethane conversion as a function of time for several samples of

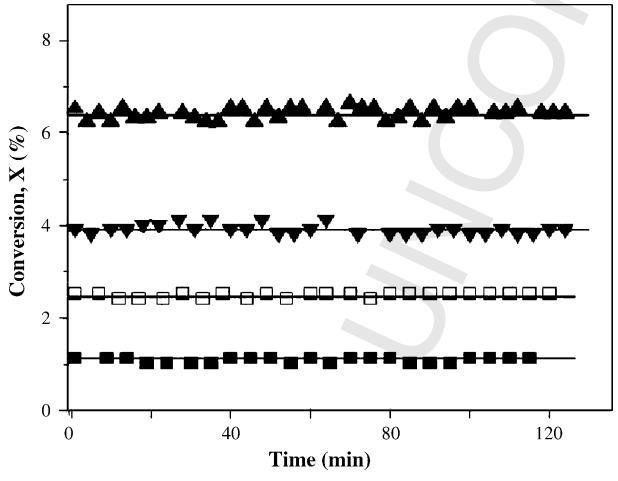

Fig. 2. Ethane conversion as a function of time. Pt/ZSM5 (▲), $W/F^0_E = 0.82\ g\,h\,mol^{-1}$; Pt/Al_2O_3 (▼), $W/F^0_E = 22.4\ g\,h\,mol^{-1}$; Pt/KL (□), $W/F^0_E = 0.70\ g\,h\,mol^{-1}$; Pt/MgO (■), $W/F^0_E = 18.4\ g\,h\,mol^{-1}$. $T = 573$ K, $P = 101.3$ kPa, ethane:O_2:N_2 = 1.8:10:88.2.

Table 1; it is observed that X_E does not change with time on stream. Similarly, no catalytic decay was observed for propane and butane oxidations, thereby indicating that no significant catalyst deactivation takes place on stream. From X versus time curves we determined the alkane combustion turnover frequencies (TOF, h^{-1}) and the values are shown in Table 2. The alkane TOF values increased following the same catalyst trend as determined from light-off curves in Fig. 1.

More fundamental kinetic data were obtained by calculating the reaction orders and activation energies for ethane combustion. Reaction orders were determined by considering for the ethane combustion rate (r_E, mol alkane $h^{-1}\,g^{-1}_{Pt}$) a power-law rate equation

$$r_E = k(P^0_E)^{\alpha}(P^0_{O_2})^{\beta} \quad (1)$$

where P^0_E and $P^0_{O_2}$ are the partial pressures of ethane and oxygen in the feed, respectively. Reaction orders α and β were determined graphically from logarithmic plots representing the r_E values as a function of P^0_E and $P^0_{O_2}$, respectively, and are presented in Table 3. The reaction order with respect to ethane was close to 1 on all the samples, while the reaction order in oxygen was negative on all the samples. The absolute value of β, however, increased with increasing sample acidity. Similar results were obtained for propane combustion [12] and are in line with previous works reporting that lower-alkanes oxidation is order zero or negative on Pt-based catalysts [9,10,17]. Lower alkane adsorption on Pt is energetically competitive with oxygen [20] and the interaction between the two competitively adsorbed reactants explains in a Langmuir–Hinshelwood mechanism the reaction inhibition by O_2 when using oxygen-rich alkane–O_2 mixtures, as is the case here.

The apparent activation energy (E_{app}) and preexponential factor A of ethane oxidation were determined using an Arrhenius-type function, by plotting ln r_E values as a function of $1/T$. Results in Table 3 show that E_{app} increased with the catalyst activity: the higher the catalyst activity, the higher the E_{app} value. A similar trend was found between preexponential factors A and catalyst activity: the most active catalyst shows the highest A value. In Fig. 3 we plotted the ln A values as a function of E_{app} in order to verify if the experimental data obey a Cremer–Constable relation [21,22]

$$\ln A = mE_{app} + c \quad (2)$$

Table 3
Kinetic results for ethane combustion

Catalyst	Activation energy, E_a (kcal mol^{-1})	Preexponential factor, A ($h^{-1}\,kPa^{-(1+\beta)}$)	Reaction orders	
			α	β
Pt/MgO	7.1	3.38×104	0.85	−0.04
Pt/Al2O3	17.4	4.86×109	1.10	−0.06
Pt/KL	19.4	6.74×109	0.84	−0.09
Pt/HY	24.1	7.06×1012	1.15	−0.38
Pt/ZSM5	27.3	2.31×1014	1.28	−0.54
Pt/Beta	34.2	4.93×1017	1.20	−0.65

$T = 533$ K, ethane:O_2:N_2 = 1.8:10:88.2, $P = 101.3$ kPa.

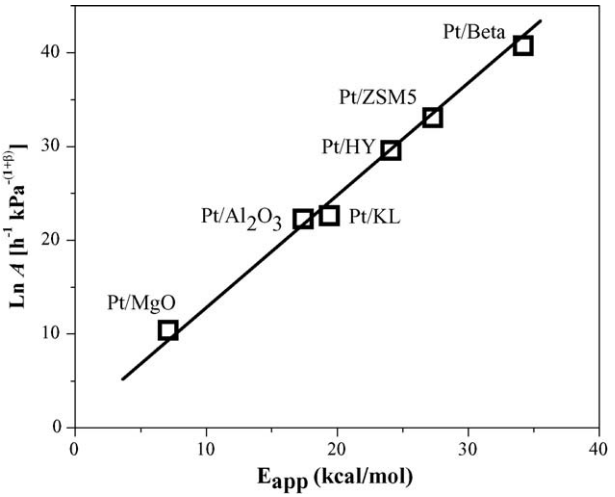

Fig. 3. Compensation effect for ethane combustion. Experimental conditions as in Fig. 2.

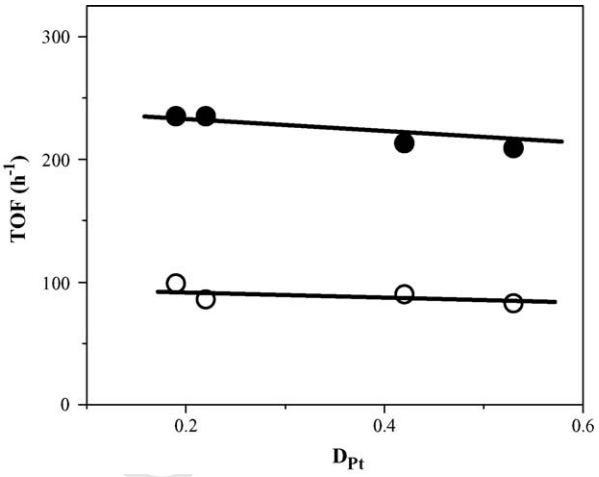

Fig. 4. Turnover oxidation rates for ethane and propane as a function of platinum dispersion on Pt/Al_2O_3. Ethane: $W/F^0_E = 22.4\ g\ h\ mol^{-1}$, $T = 573$ K, $P = 101.3$ kPa, ethane:O_2:N_2 = 1.8:10:88.2. Propane: $W/F^0_P = 58.0\ g\ h\ mol^{-1}$, $T = 533$ K, $P = 101.3$ kPa, propane:O_2:N_2 = 0.8:9.9:89.3.

A linear plot was obtained thereby indicating that a compensation phenomenon took place. Compensation was also observed for propane combustion [13]. The existence of a compensation phenomenon for ethane oxidation is qualitatively consistent with the X versus T curve shapes shown in Fig. 1A. In fact, as it was reported [12], the $x = f(T)$ function obtained from the design equation of a plug-flow integral reactor and a reaction rate with $\alpha = 1$ and $\beta = 0$, predicts that the sigmoidal light-off curve becomes sharper and is shifted to lower temperatures by increasing A, in spite of the simultaneous increasing of the apparent activation energy. This is exactly what it is observed in Fig. 1A and is consistent with the usual positive compensation in which the trend of $\ln A$ with E_{app} is sympathetic.

In summary, our catalytic results, in particular those in Table 2, show that C_2–C_4 alkane oxidation turnover rates are about two (ethane, propane) and one (butane) orders of magnitudes higher on Pt/acid zeolites than on Pt/Al_2O_3 that has been widely employed as a reference catalyst for hydrocarbon combustion. But the alkane combustion turnover rates are also significantly higher on weakly acid PtKL zeolite as compared to Pt/Al_2O_3 (more than one order of magnitude for ethane and propane). In order to explain such a drastic increase of the Pt oxidation activity when the metal is supported on zeolites, we investigated different factors that may influence the intrinsic metal oxidation activity.

3.3. Effect of Pt crystallite size

We first studied the effect that changing $\bar{d}_{Pt}$ has on the metal activity because previous reports have shown that the activity for hydrocarbon combustion may be strongly dependent on the mean metal particle size. For example, we have found [23,24] that turnover rates for benzene and cyclopentane oxidations on Pt/Al_2O_3 increase more than one order of magnitude when $\bar{d}_{Pt}$ is increased from about 15 to 50 Å. Recent papers confirmed that the aromatic hydrocarbon combustion on Pt-based catalysts is preferentially promoted on larger metal particles [25,26]. Here, we investigated the structure sensitivity of alkane combustion on Pt/Al_2O_3, Pt/HY and Pt/Beta samples by changing the metal particle size by sintering. Ethane and propane oxidation turnover rates were determined on Pt/Al_2O_3, Pt/Al_2O_3-1, Pt/Al_2O_3-2, and Pt/Al_2O_3-3 samples (Table 1) and the obtained TOF values are plotted as a function of Pt dispersion in Fig. 4. We do not observe any significant change for $TOF_{E(P)}$ with increasing Pt particle size in Fig. 4, which is in line with previous studies performed for the total oxidation of C_1–C_4 n-alkanes on Pt/Al_2O_3 [27]. We also prepared two sintered Pt/HY and Pt/Beta samples by treating the corresponding fresh Pt/zeolites for 4 h at 773 K, in an $O_2(2\%)/N_2$ gaseous mixture. It was verified that this sintering treatment does not change significantly neither the acidity nor the surface area of the zeolites. Propane oxidation was carried out on fresh and sintered Pt/HY and Pt/Beta samples and the results are presented in Table 4. Only a sligth decrease of the TOF_P value was observed when the Pt dispersion diminished from 30 to 15% on Pt/HY, and from 41 to 17% on Pt/Beta. From the results of Fig. 4 and Table 4 we must conclude that lower alkane oxidation is not a demanding reaction on Pt when the metal is supported on alumina or acid zeolites. The differences in the alkane oxidation turnover rates shown in Table 2 cannot be explained therefore by any change of the Pt crystallite size.

Table 4
Effect of Pt dispersion on propane oxidation turnover rates over Pt/zeolite catalysts

Catalyst	Fresh		Sintered	
	D_{Pt} (%)	TOF (h^{-1})	D_{Pt} (%)	TOF (h^{-1})
Pt/HY	30	10550	15	6900
Pt/Beta	41	3900	17	2700

523 K (Pt/HY), 488 K (Pt/Beta), $P = 101.3$ kPa, propane:O_2:N_2 = 0.8:9.9:89.3.

3.4. Effect of the addition of water

We also investigated if the formation of water during reaction may modify the intrinsic Pt activity for hydrocarbon oxidation, taking into account that zeolites are more hydrophylic materials than Al_2O_3 or MgO. Specifically, propane oxidation was carried out on Pt/HY and Pt/Al_2O_3 samples and 0.24% water was added to the feed during the reaction for about 60 min (Fig. 5). This water concentration corresponded approximately to the water amount formed for 8% propane conversion. Thus, the water concentration added to the feed was in the order of that formed during the standard X versus T catalytic runs performed for measuring the sample turnover rates (Fig. 2). Qualitatively, similar behavior was observed on both samples: the presence of water decreases the catalyst activity because hydrocarbon oxidation on Pt is negative order in water, but the initial conversion is recovered after water elimination in the feed. No substantial difference regarding the effect of water on the oxidation activity is observed when comparing both samples. This result strongly suggests that formation of water on stream is not responsible for the significant difference of the alkane oxidation turnover rate observed when comparing Pt/HY and Pt/Al_2O_3 samples (Table 2).

3.5. Effect of suport acidity

Differences in the support acid strength may influence the intrinsic oxidation Pt activity. Yazawa et al. studied the propane combustion on Pt supported on different supports [9,10,28], namely MgO, Al_2O_3, ZrO_2, SiO_2, SiO_2–Al_2O_3, and SO_4–ZrO_2. They also studied the additive effect for propane combustion on Pt/Al_2O_3 by incorporating to the support several additives of different electronegativity [11]. Their results showed that the propane oxidation activity on platinum increased with the acid strength of support and the electronegativity of additives. In basis of catalyst characterization results obtained by EXAFS spectroscopy [29], they postulated that under oxidizing conditions the oxidation-resistance of platinum is enhanced on electrophilic supports, thereby increasing the Pt combustion activity. Besides, the propane oxidation turnover rate will increase with decreasing Pt dispersion because platinum in large particles would be less oxidized than in smaller ones [10]. The light-off curves obtained for the combustion of ethane and butane in Fig. 1 show that the Pt activity increases following qualitatively the sample capacity for adsorbing ammonia (Table 1). However, quantitative kinetic results obtained in catalytic tests conducted at low conversions and constant temperature show in Table 2 that the TOF values for alkane oxidation are dramatically higher on Pt/KL as compared to Pt/Al_2O_3 (more than one order of magnitude for ethane and propane, and a factor of three for butane), despite that both samples exhibit similar acidity (Table 1). It is then apparent that the abrupt increase of the Pt activity for alkane oxidation observed when comparing Pt/KL with Pt/Al_2O_3 cannot be explained in terms of density of surface acid sites. On the other hand, our results for ethane combustion show that the negative order with respect to oxygen increases with increasing support acidity (Table 3); similar trend was observed for propane combustion [12]. These results are not consistent with the interpretation that Pt on electrophilic supports has the higher oxidation-resistance. In fact, if the effect of the acid supports is to prevent Pt from oxidation it is expected that the inhibition by oxygen would decrease with the support acid strength. Besides, and contrary to the claims of Yasawa et al. [10], we do not observe any significant effect of the Pt crystallite size on the oxidation turnover rates, either when supported on alumina (Fig. 4) or in zeolite HY (Table 4). In summary, from our results we conclude that the support acidity is not the major contributing factor for explaining the drastic alkane oxidation activity enhancement determined on Pt/zeolites as compared to Pt/Al_2O_3. This conclusion is in line with previous studies on propane oxidation over Pt supported on non-zeolitic materials, which did not find any correlation between the catalyst activity and the total acidity of the support [4,5].

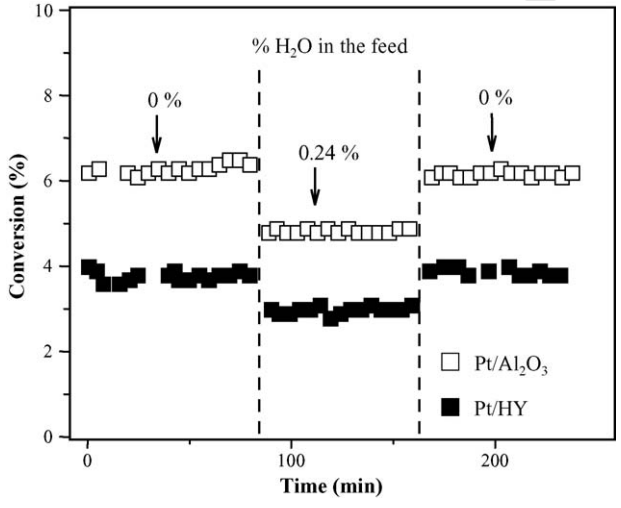

Fig. 5. Propane combustion: effect of the addition of water. $T = 533$ K, $P = 101.3$ kPa, propane:O_2:N_2 = 0.8:9.9:89.3, Pt/Al_2O_3: $W/F^0_P = 58.0\ g\,h\,mol^{-1}$, Pt/HY: $W/F^0_P = 1.0\ g\,h\,mol^{-1}$.

3.6. Effect of the support alkane uptake capacity

In a previous paper [12], we determined the propane uptake capacity at room temperature for the same samples used in this work. We found that the areal propane uptake measured on Pt/KL at 0.8 kPa (the feed propane pressure used in catalytic tests) was one order of magnitude higher than on Pt/MgO and Pt/Al_2O_3 and realized that a drastic increase of the density of propane adsorbed species under reaction may promote the alkane oxidation rate. We measured here, then, the ethane and butane uptake capacities of the samples at room temperature and 0.8 kPa. Results are given in Table 5; for comparison, we have also included in Table 5 the propane uptake values. It is observed that the areal uptake for the three alkanes on Pt/Al_2O_3 is about two orders and one order of magnitude lower than on Pt/acid zeolites and Pt/KL, respectively. The ability of zeolites to concentrate reactant molecules was recognized as sorption [30] or confinement [31] effects. The increase of the average reactant concentration in the zeolite cavities arises in the

Table 5
Alkane uptakes over Pt-supported catalysts

Catalyst	Alkane uptake (μmol m^{-2})[a]		
	Ethane	Propane	Butane
Pt/MgO	0.059	0.011	0.090
Pt/Al_2O_3	0.025	0.035	0.086
Pt/KL	0.520	0.420	0.584
Pt/HY	1.100	0.820	0.725
Pt/ZSM5	1.520	1.020	1.130
Pt/Beta	1.465	0.910	0.850

[a] Values determined at $P = 0.80$ kPa. The adsorption isotherms were carried out at room temperature.

confinement model [31,32] from the van der Waals interactions between the adsorbate and the zeolite framework, and is interpreted in basis of three main parameters: the diameter of the zeolites pores, the polarizabilities of the zeolite framework and of the adsorbate, and the critical adsorbate dimension [32,33]. The drastic increase of the alkane uptake capacity shown for Pt/zeolite samples in Table 5 would reflect the alkane confinement into the zeolite pores and probably explains the alkane oxidation rate enhancement observed on Pt/zeolites. According to literature [15,16,19], the rate-determining step of the alkane oxidation mechanism on platinum is the dissociative chemisorption of the alkane on Pt with the breakage of the weakest C–H bond followed by its interaction with oxygen atoms adsorbed on adjacent sites. A direct consequence of increasing the local alkane concentration around the metallic Pt active sites would be the increase of the alkane oxidation conversion rate because the reaction is positive order with respect to the hydrocarbon, close to one (Table 4).

On the other hand, the effect of confinement has also been employed for interpreting changes in the apparent activation energies observed for paraffin cracking on zeolites by considering that E_{app} comprises an enthalpy term corresponding to the physical adsorption of the adsorbate in the zeolite cavities [34]. Specifically, confinement explained the differences in E_{app} when the cracking of linear hydrocarbons of variable chain was carried out on a given zeolite [35]. We observed here that E_{app} for C_2–C_4 alkane oxidations increases following qualitatively a similar trend than both the C_2–C_4 alkane uptakes and the catalyst oxidation activity. As we stated above, the parallel increase of the catalyst oxidation activity and E_{app} was verified because experimental data obeyed a Constable relationship $\ln A = mE_{app} + c$, and the positive kinetic effect of increasing the preexponential factor A compensates the E_{app} augmentation. Taking into account that the increase of A would reflect an increase of the number of active sites, we proposed in a previous work [12] that the high density of hydrocarbon species adsorbed on the zeolite support may give rise to an additional oxidation reaction pathway that would take place between the alkane species adsorbed in the metal-oxide interfacial region and the oxygen spilled-over from Pt. Alkane oxidation via this later mechanism would be promoted by the density increase of adsorbed alkane molecules in the interfacial region as a consequence of the alkane confinement in zeolite micropores. A similar model considering that the overall activity can be separated into that from the metal surface and that from the interfacial region has been proposed for explaining the aromatic hydrocarbon hydrogenation rate enhancement obtained on Pt supported on acid materials as compared to Pt/SiO_2 catalysts [36,37].

In summary, the origin of the superior activity of Pt/zeolites for the combustion of C_2–C_4 alkanes seems to be related with the ability of zeolites for increasing the alkane concentration in zeolite cavities. The higher alkane partial pressure in zeolite micropores would increase the alkane oxidation rate because the reaction is positive order with respect to the hydrocarbon, but probably also because increases the number of active sites via an additional oxidation pathway that takes place in the metal-oxide interfacial region and activates the alkane C–H bond. The presence of activation sites for C–H bonds in the neighborhood of platinum oxide crystallites which release oxygen species at a high rate, i.e. PtOx is reduced and oxidized at a high rate, would contribute to the improved performance of Pt/zeolite samples.

4. Conclusions

The combustions of ethane, propane and butane on Pt supported on MgO, alumina, and zeolites KL, HY, ZSM5, and Beta exhibit a similar catalytic behavior characterized by: (i) the reaction is structure insensitive on Pt, irrespective of the support employed; (ii) the reaction is about first order with respect to the alkane and negative order in oxygen; (iii) more active catalysts exhibit higher apparent activation energies because a compensation effect is verified between the apparent activation energy and the preexponential factor. But the most significant common factor for the combustion of C_2–C_4 alkanes is that the Pt oxidation activity is drastically increased when supported on zeolites as compared to Pt/Al_2O_3 or Pt/MgO. This superior activity of Pt/zeolites for lower alkane combustion is probably caused by the alkane confinement in the zeolite micropores. The enhanced alkane concentration in zeolite cavities increases the alkane combustion rate because the reaction is positive order in the hydrocarbon and probably also because increases the density of adsorbed alkane in the metal-oxide interfacial region.

References

[1] J.J. Spivey, Ind. Eng. Chem. Res. 26 (1987) 2165.
[2] K.T. Chuang, S. Cheng, S. Tong, Ind. Eng. Chem. Res. 31 (1992) 2466.
[3] H.C. Yao, H.K. Stephen, H.S. Gandhi, J. Catal. 67 (1981) 237.
[4] C.P. Hubbard, K. Otto, H.S. Gandhi, K.Y. Ng, J. Catal. 144 (1993) 484.
[5] R. Burch, E. Halpin, M. Hayes, K. Ruth, J.A. Sullivan, Appl. Catal. B: Environ. 19 (1998) 199.
[6] A.F. Lee, K. Wilson, R. Lambert, C.P. Hubbard, R.G. Hurley, R.W. McCabe, H.S. Gandhi, J. Catal. 184 (1999) 491.
[7] A. Hinz, M. Skoglundh, E. Fridell, A. Andersson, J. Catal. 201 (2001) 247.
[8] G. Corro, J.L.G. Fierro, V.C. Odilon, Catal. Commun. 4 (2003) 371.
[9] Y. Yazawa, N. Kagi, S. Komai, A. Satsuma, Y. Murakami, T. Hattori, Catal. Lett. 72 (2001) 157.
[10] Y. Yasawa, H. Yoshida, T. Hattori, Appl. Catal. A: Gen. 237 (2002) 139.
[11] Y. Yasawa, H. Yhosida, S. Komai, T. Hattori, Appl. Catal. A: Gen. 233 (2002) 113.

[12] T.F. Garetto, E. Rincón, C.R. Apesteguía, Appl. Catal. B: Environ. 48 (3) (2004) 167.
[13] J.I. Di Cosimo, V. Díez, C.R. Apesteguía, Appl. Catal. 137 (1996) 149.
[14] L. Spenadel, M. Boudart, J. Phys. Chem. 64 (1960) 204.
[15] L. Hiam, H. Wise, S. Chaikin, J. Catal. 10 (1968) 272.
[16] M. Aryafar, F. Zaera, Catal. Lett. 48 (1997) 173.
[17] R. Burch, T.C. Watling, J. Catal. 169 (1997) 45.
[18] V.P. Zhdanov, B. Kasemo, J. Catal. 195 (2000) 46.
[19] T.F. Garetto, C. Apesteguía, in: A. Corma, F. Melo, S. Mendorioz, J.L.G. Fierro (Eds.), Studies in Surface Science and Catalysis, vol. 130, Elsevier, Amsterdam, 2000, p. 575.
[20] Y.Y. Yao, Ind. Eng. Chem. Prod. Res. Dev. 19 (1980) 293.
[21] F.H. Constable, Proc. Roy. Soc. (London) 108 (1925) 355.
[22] E. Cremer, Z. Phys. Chem. 144 (1929) 231.
[23] T.F. Garetto, C.R. Apesteguía, Catal. Today 62 (2–3) (2000) 189.
[24] T.F. Garetto, C.R. Apesteguía, Appl. Catal. B: Environ. 32 (1–2) (2001) 83.
[25] F.J. Maldonado-Hódar, C. Moreno-Castilla, A.F. Pérez-Cadenas, Appl. Catal. B: Environ. 61 (2005) 277.
[26] M.N. Padilla-Serrano, F.J. Maldonado-Hódar, C. Moreno-Castilla, Appl. Catal. B: Environ. 61 (2005) 277.
[27] Y.Y. Yao, Ind. Eng. Chem. Prod. Res. Dev. 19 (1980) 293.
[28] Y. Yazawa, H. Yoshida, N. Takagi, N. Kagi, S. Komai, A. Satsuma, Y. Murakami, T. Hattori, in: A. Corma, F. Melo, S. Mendorioz, J.L.G. Fierro (Eds.), Studies in Surface Science and Catalysis, vol. 130, Elsevier, Amsterdam, 2000, p. 2189.
[29] H. Yoshida, Y. Yasawa, N. Takagi, A. Satsuma, T. Tanaka, S. Yoshida, T. Hattori, J. Synchrotron Rad. 6 (1999) 471.
[30] W.O. Haag, Stud. Surf. Sci. Catal. 84 (1994) 1375.
[31] E.G. Derouane, J.M. Andre, A.A. Lucas, J. Catal. 110 (1088) 58.
[32] E.G. Derouane, Chem. Phys. Lett. 142 (1987) 200.
[33] P. Lambin, A.A. Lucas, I. Derijcke, J.P. Vigneron, E.G. Derouane, J. Phys. Chem. 40 (1989) 3814.
[34] E.G. Derouane, C.D. Chang, Micropor. Mesopor. Mater. 35–36 (2000) 425.
[35] R.J. Gorte, D. White, Micropor. Mesopor. Mater. 35–36 (2000) 447.
[36] S.D. Lin, M.A. Vannice, J. Catal. 143 (1993) 539.
[37] S.D. Lin, M.A. Vannice, J. Catal. 143 (1993) 554.